# Inner-valence states of $N_2^+$ studied by uv photoelectron spectroscopy and configuration-interaction calculations

P. Baltzer
*Department of Physics, Uppsala University, Box 530, S-75121 Uppsala, Sweden*

M. Larsson
*Department of Physics 1, Royal Institute of Technology, S-10044 Stockholm, Sweden*

L. Karlsson, B. Wannberg, and M. Carlsson Göthe
*Department of Physics, Uppsala University, Box 530, S-75121 Uppsala, Sweden*

(Received 11 May 1992)

He II–excited inner-valence photoelectron spectra of the nitrogen molecule have been recorded between 23 and 35 eV using a spectrometer resolution of better than 20 meV. In this range several photoelectron bands associated with transitions to cationic states are observed. Extensive vibrational structure has been observed in three bands, two in the (23–27)-eV range, and the third in the (31–32)-eV range. For the well-known $C\,^2\Sigma_u^+$ state, a substantial potential barrier towards dissociation has been found. The second vibrational progression in the (23–27)-eV range has very small vibrational spacings, on the order of 86 meV, and is associated with the second state of $^2\Pi_g$ symmetry. Transitions to the first state of this symmetry, $D\,^2\Pi_g$, are found to give rise to a continuous band above the dissociation threshold. The third vibrational progression is tentatively assigned to the $3\,^2\Sigma_g^+$ state. The assignments are supported by complete-active-space self-consistent-field and multireference configuration-interaction calculations on the $D\,^2\Pi_g$, $2\,^2\Pi_g$, $F\,^2\Sigma_g^+$, and $3\,^2\Sigma_g^+$ states, and potential curves have been computed in good agreement with the observations.

PACS number(s): 32.80.Fb, 31.20.Tz

## I. INTRODUCTION

The nitrogen molecule is one of the most important diatomic systems due to its ubiquitous presence in the atmosphere. A good understanding of its electronic structure and photoionization dynamic properties is therefore of fundamental interest. In particular, transitions to the inner valence states of $N_2^+$ often lead to dissociation of the system with consequent formation of atomic radicals.

The inner-valence region in the photoelectron spectrum of the nitrogen molecule has been the subject of several earlier studies. Ultraviolet photoelectron spectra were obtained by Åsbrink and Fridh [1] and Potts and Williams [2] using He II radiation, and by Krummacher, Schmidt, and Wuilleumier [3] using synchrotron radiation. More recently, high resolution x-ray photoelectron spectra (XPS) covering the inner-valence region between 20 and 45 eV were presented [4] and assigned by comparison to resonance Auger [or deexcitation-spectroscopy (DES)] spectra [5] and the results of extensive configuration-interaction (CI) calculations of photoelectron intensities at one internuclear distance [6].

In the present investigation we have recorded He II–excited photoelectron spectra in the energy range between 20 and 35 eV. The study has been carried out using an improved uv source with very good characteristics, which has allowed recordings with both high resolution and intensity, despite a low photoionization cross section for He II radiation [7]. Some of the recordings were carried out with monochromatic He II $\alpha$ radiation using a newly designed monochromator [8], which acts as a filter for the different components of the resonance radiation produced by the uv source. Extensive vibrational structures associated with three different electronic states have been observed in the spectrum. These structures provide information that is useful for discussing the potential curves of the electronic states and for comparison with theoretical results.

Potential curves have previously been calculated using *ab initio* methods for many of the inner-valence states of $N_2^+$. Some of these were carried out already in the 1970s [9–11], and were of reasonable accuracy. More recently a number of studies have been performed using more advanced methods [12, 13]. These adiabatic potential curves are complex, and in many cases exhibit high barriers towards dissociation due to interaction between states of the same symmetry. In the present investigation we have carried out calculations of potential curves of the two lowest states of $^2\Pi_g$ symmetry, called $D\,^2\Pi_g$ and $2\,^2\Pi_g$, and, in addition, two states of $^2\Sigma_g^+$ symmetry, the $F$ state, which is observed in the (27–29)-eV range, and the third state of this symmetry appearing in the energy range above 30 eV. The accuracy obtained in these calculations is similar to recent calculations on states of $^2\Sigma$, $^2\Delta$, and $^4\Pi$ symmetry [13] in the same energy range, and we have used all these results in the present study to make an analysis of the electronic states in the range between 22 and 33 eV and to provide an interpretation of the photoelectron spectrum.

 

## II. EXPERIMENTAL DETAILS

The measurements were performed by means of a uv photoelectron spectrometer that has been described in some detail previously [14]. Briefly, it is based on an electrostatic hemispherical analyzer with a mean radius of 144 mm and a microchannel plate detector system. An electron lens focuses the photoelectrons onto the entrance slit of the analyzer. The target-gas molecules are let into a gas cell where the photoionization takes place. Target-gas pressures on the order of a few mtorr were used in the present investigation. By a recent redesign of the gas cell, we have managed to practically eliminate the processes that normally lead to a background intensity in the photoelectron spectra [15]. By further improvements, the leakage of He gas into the gas cell, which inevitably leads to the presence of a helium line in spectra at 24.587 eV, has been considerably reduced in many spectra. In addition, using a correction electrode arrangement [15], potential gradients inside the gas cell, which normally tend to broaden the lines, have been reduced to an insignificant level.

The He II $\alpha$ radiation that has been employed for the photoionization was produced in a vacuum ultraviolet (vuv) source based on a microwave electron-cyclotron-resonance (ECR) discharge [16]. The discharge takes place at a pressure of about 50 mtorr in a very small volume between the poles of a strong magnet, which provides a field acting as a magnetic bottle that fulfills the ECR condition in the center. This source gives a high He II $\alpha$ intensity that makes detailed studies of the inner-valence region feasible. Furthermore, the linewidth of this radiation is very small (on the order of 1 meV). This uv source has recently been made commercially available.

The sample gas was obtained commercially with a purity of better than 99.99%. The calibration of the spectra was done by using the He line at 24.587 eV as the energy reference. The resulting accuracy in the determination of binding energies for well-defined lines is better than $\pm 2$ meV.

All spectra are presented as originally obtained from the spectrometer, i.e., no deconvolution or background subtraction has been made. The vibrationally resolved spectra are complex, and in order to determine the energies, full widths at half maxima (FWHM), and relative intensities of the individual vibrational components, a curve fitting has been performed where Gaussian lines were fitted to the observed spectrum. This procedure was carried out using a spreadsheet program (EXCEL) which was run on a Macintosh Quadra 700 computer in collaboration with Apple Computer AB in Sweden.

## III. COMPUTATIONAL METHODS

Complete-active-space self-consistent-field (CASSCF) [17] and multireference CI (MRCI) [18] calculations were performed for some electronic states of $N_2^+$ of particular interest for the analysis of the photoelectron spectrum. The nitrogen basis set was derived from the Dunning-Huzinaga [19,20] 10*s*,6*p* set contracted to 5*s*,4*p*. The *s*,*p* basis was extended by replacing the last two *s* exponents by 3 and the last three *p* exponents by 4. Two *d* functions and one *f* function were added to the *s*,*p* set to form a contracted [6*s* 5*p* 2*d* 1*f*] basis set.

The 2*s* and 2*p* orbitals and electrons were active in the CASSCF calculations. In the CI step in the CASSCF procedure, the five and seven lowest roots of $^2\Pi_g$ and $^2\Sigma_g^+$ states were obtained. The calculations were performed in $D_{2h}$ symmetry, but $D_{\infty h}$ symmetry was imposed on the CASSCF wave functions. Since $^2\Delta_g$ and $^2\Sigma_g^+$ states are in the same $D_{2h}$ irreducible representation, calculations of $^2\Delta_g$ were carried out in two symmetries in order to separate them from $^2\Sigma_g^+$. In the MRCI calculations, the 2*s* and 2*p* electrons were correlated and the two 1*s* core orbitals were doubly occupied. Only selected configurations from the CASSCF wave functions were included in the reference list. The criterion was that a configuration should have a coefficient larger than 0.05 at some internuclear distance. The MRCI calculations were carried out for the $D\ ^2\Pi_g$, $2\ ^2\Pi_g$, $F\ ^2\Sigma_g^+$, and $3\ ^2\Sigma_g^+$ states.

The accuracy in the present calculations is expected to be close to that of Refs. [12] and [13]. In order to test this, we also carried out a calculation of the $X\ ^2\Sigma_g^+$ state at one internuclear distance. The result was within 0.1 eV of that of Ref. [12].

## IV. RESULTS

For completeness, an overall spectrum was recorded in the present study using monochromatic He II $\alpha$ radiation. This spectrum is shown in Fig. 1. The well-known outer-valence photoelectron spectrum is seen between 15.5 and 20 eV. It corresponds to ionization from the three outermost orbitals in the electron configuration, written as

$$1\sigma_g^2 1\sigma_u^2 2\sigma_g^2 2\sigma_u^2 1\pi_u^4 3\sigma_g^2 .$$

Ionization from the inner-valence $2\sigma_g$ orbital, leading to a manifold of lines in x-ray photoelectron spectra between 36 and 41 eV [4], is probably reflected by the weak

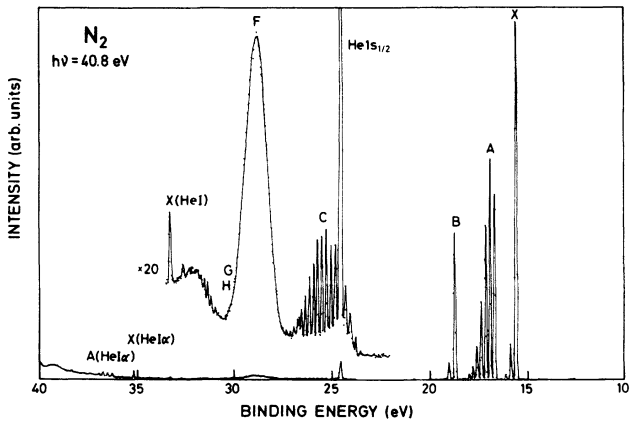


FIG. 1. The valence photoelectron spectrum of the $N_2$ molecule excited by monochromatic He II $\alpha$ radiation. Assignments of the photoelectron bands are given in terms of the final cationic states reached in the transitions.

feature centered at 39 eV.

In the range between 20 and 35 eV, a number of weak bands are observed, corresponding to inner-valence electron correlation states. A summary of the observed adiabatic and vertical binding energies for these bands is given in Table I, along with assignments in terms of the ionic states reached in the photoelectron transitions. These assignments differ on some points from those made in our earlier study [4] as a result of the additional information obtained in the present investigation. This will be further discussed in the following.

The relative intensities of the vibrational lines seen in Fig. 1 follow the expected behavior for Franck-Condon transitions. However, recent studies carried out using He I $\alpha$ excitation and a very high signal-to-background ratio indicate that, in this spectrum, very weak vibrational structure associated with the outer-valence single-hole states can be observed over the entire spectrum up to the energy limit at 21.22 eV. This resembles earlier observations of such extended vibrational structure made for the CO molecule [21,22], and will be the subject of a separate report.

Figure 2 shows a more detailed recording of the inner-valence band observed around 25 eV. A long vibrational progression can be seen, which starts at 23.6 eV and has its maximum intensity at 25.5 eV. The vibrational energies are collected in Table II, along with the relative intensities obtained from a curve-fitting procedure. The progression fits well with the $C\,^2\Sigma_u^+$ state observed already by Gilmore [23]. This assignment has been confirmed by experimental studies [4] and extensive calculations [6,10,11,13,24–26], which have associated this state with a leading $3\sigma_g^{-1}1\pi_u^{-1}1\pi_g^1$ electron configuration at short internuclear distances. The first peak observed at 23.583 eV provides an adiabatic binding energy that is in very good agreement with the value given in Ref. [23]. This peak is seen clearly in Fig. 3, which shows a separate recording of the first part of the band.

The vibrational progression can be followed up to $v=18$, where the overlap with the next band makes further identification difficult. This region was therefore studied separately with better statistics. Figure 4 shows

TABLE I. Summary of the observed states of $N_2^+$ in Fig. 1. The vertical binding energies refer to the maximum intensity of the photoelectron band.

| Electronic state | Adiabatic binding energy (eV) | Vertical binding energy (eV) |
|---|---|---|
| $X\,^2\Sigma_g^+$ | 15.580 | 15.580 |
| $A\,^2\Pi_u$ | 16.693 | 16.926 |
| $B\,^2\Sigma_u^+$ | 18.751 | 18.751 |
| $C\,^2\Sigma_u^+$ | 23.583 | 25.514 |
| $2\,^2\Pi_g$ | 23.755 | 24.788 |
| $D\,^2\Pi_g$ | | 26 |
| $F\,^2\Sigma_g^+$ | | 28.8 |
| $G\,^2\Pi_u$ | | 30 |
| $H\,^2\Pi_u$ | | 30 |
| $3\,^2\Sigma_g^+$ | | 31.01 |

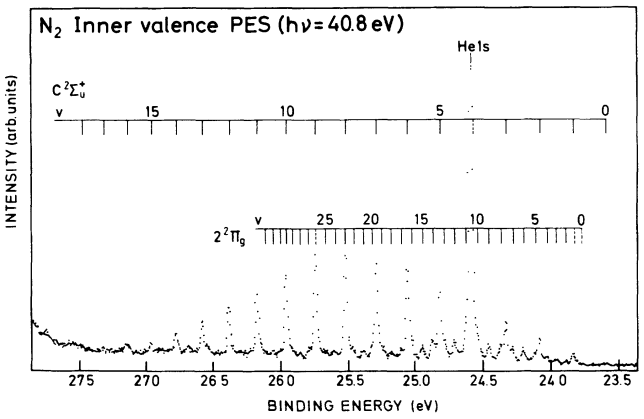


FIG. 2. High-resolution recording of the inner-valence region of the He II–excited $N_2$ photoelectron spectrum (PES) between 23 and 28 eV. Two vibrational progressions are indicated. The strong progression is associated with transitions to the $C\,^2\Sigma_u^+$ state, and the weaker to the $2\,^2\Pi_g$ state.

the result of such a recording. It exhibits narrow lines up to $v=15$, whereas the $v=16$ line seems to be broadened. The widths (FWHM) obtained for these lines are 32 and 40 meV, respectively. The $v=18$ component is not resolved since it is overlapped by new lines that start to appear on the slope of the next intense band centered at 28.8 eV (cf. Table I). Another observation that can be made is a background enhancement over the region of

TABLE II. Vibrational energy levels for the $C\,^2\Sigma_u^+$ state of $N_2^+$ and relative intensities (peak areas) in transitions from the neutral ground state.

| Vibrational quantum number $v$ | Binding energy (eV) | Vibrational spacing (meV) Expt. | Vibrational spacing (meV) Theory [13] | Relative intensity |
|---|---|---|---|---|
| 0 | 23.583 | | | 0.024 |
| 1 | 23.831 | 248 | 253.3 | 0.10 |
| 2 | 24.083 | 252 | 251.5 | 0.25 |
| 3 | 24.331 | 248 | 247.9 | 0.41 |
| 4 | 24.576[a] | | 243.8 | |
| 5 | 24.817 | | 239.6 | 0.69 |
| 6 | 25.054 | 237 | 235.3 | 0.87 |
| 7 | 25.286 | 232 | 230.8 | 0.96 |
| 8 | 25.514 | 228 | 226.1 | 1.00 |
| 9 | 25.738 | 224 | 221.3 | 0.98 |
| 10 | 25.956 | 218 | 216.0 | 0.76 |
| 11 | 26.171 | 215 | 210.5 | 0.59 |
| 12 | 26.378 | 207 | 204.2 | 0.47 |
| 13 | 26.580 | 202 | 196.7 | 0.33 |
| 14 | 26.778 | 198 | 186.2 | 0.22 |
| 15 | 26.965 | 187 | 168.5 | 0.14 |
| 16 | 27.146 | 181 | | 0.12 |
| 17 | 27.322 | 176 | | 0.05 |
| 18 | 27.478 | 158 | | 0.04 |

[a]Interpolated value. The line is unobserved due to the overlap with the He 1$s$ line.

the *C* state (cf. Figs. 1 and 2) that cannot be explained satisfactorily by overlapping vibrational structure. It seems to start at about 24 eV, and could therefore reflect the presence of a dissociation continuum in the energy range between 24.3 and 27 eV. A similar and even more pronounced enhancement of the intensity is seen in the $N^+$ photoion spectrum [27]. An interpretation of these observations is suggested in the discussion.

In Figs. 2 and 3, numerous weak peaks can be observed in the (24–26)-eV range, superimposed on the structures belonging to the *C* state. The energies and relative intensities are given in Table III. These peaks are about 35% broader than those of the *C* state, and seem to form a long vibrational progression with very small spacings decreasing from about 85 meV in the first part of the band to about 50 meV in the 26-eV region. However, the spacings between the first few components are substantially smaller than between the following lines. Well-resolved components of this progression are observed also in the spectrum induced by monochromatic He II $\alpha$ radiation, shown in Fig. 1, which excludes satellite radiation from the uv source as an explanation. Therefore, these lines must reflect energy levels in $N_2^+$. Despite the overlap with the lines corresponding to the *C* state, most of the

TABLE III. Vibrational energy levels for the $2\,^2\Pi_g$ state of $N_2^+$ and relative intensities (peak areas) in transitions from the neutral ground state. The intensities are normalized to the highest peak of the *C*-state progression (cf. Table II).

| Vibrational quantum number $v$ | Binding energy (eV) | Vibrational spacing (meV) | | | Relative intensity (Expt.) |
|---|---|---|---|---|---|
| | | Expt. | Theory | | |
| | | | (b) | (c) | |
| 0 | 23.755 | | | | 0.011 |
| 1 | 23.809 | 54 | 40.0 | 48.2 | 0.032 |
| 2 | 23.881 | 72 | 63.5 | 64.8 | 0.040 |
| 3 | 23.957 | 76 | 74.7 | 81.9 | 0.069 |
| 4 | 24.032 | 75 | 79.9 | 87.2 | 0.10 |
| 5 | 24.117 | 85 | 83.4 | 90.2 | 0.15 |
| 6 | 24.202 | 85 | 85.2 | 91.6 | 0.21 |
| 7 | 24.287 | 85 | 86.4 | 92.1 | 0.23 |
| 8 | 24.370 | 83 | 86.6 | 92.1 | 0.25 |
| 9 | 24.456 | 86 | 86.5 | 91.7 | 0.25 |
| 10 | 24.541 | 85 | 86.0 | 90.8 | 0.28 |
| 11 | 24.627 | 86 | 85.2 | 89.5 | 0.29 |
| 12 | 24.710 | 83 | 84.2 | 88.0 | 0.30 |
| 13 | 24.788 | 78 | 82.9 | 86.3 | 0.31 |
| 14 | 24.865 | 77 | 81.6 | 84.5 | 0.29 |
| 15 | 24.945 | 80 | 80.1 | 82.7 | 0.23 |
| 16 | 25.025 | 80 | 78.7 | 81.0 | 0.23 |
| 17 | 25.105 | 80 | 77.2 | 79.2 | 0.17 |
| 18 | 25.175 | 70 | 75.7 | 77.5 | 0.13 |
| 19 | 25.243 | 68 | 74.2 | 75.7 | 0.17 |
| 20 | 25.320 | 77 | 72.7 | 74.0 | 0.14 |
| 21 | 25.393 | 73 | 71.2 | 72.3 | 0.13 |
| 22 | 25.467 | 74 | 69.8 | 70.6 | 0.15 |
| 23 | 25.535 | 68 | 68.3 | 68.9 | 0.14 |
| 24 | 25.600 | 65 | 66.8 | 67.2 | 0.11 |
| 25 | 25.667 | 67 | 65.3 | 65.5 | 0.10 |
| 26 | 25.730[a] | | 63.7 | 63.7 | |
| 27 | 25.793 | | 62.2 | 61.9 | 0.11 |
| 28 | 25.857 | 64 | 60.0 | 60.1 | 0.08 |
| 29 | 25.910 | 53 | 59.0 | 58.2 | 0.09 |
| 30 | 25.960 | 50 | 57.3 | 56.3 | 0.09 |
| 31 | 26.007 | 47 | 55.6 | 54.2 | 0.08 |
| 32 | 26.055 | 48 | 53.7 | 52.0 | 0.07 |
| 33 | 26.105 | 50 | 51.8 | 49.6 | 0.06 |
| 34 | 26.155 | 50 | 49.7 | 47.1 | 0.06 |

[a]This value has been interpolated. The line is unobserved due to an overlap with the $v=9$ line of the $C\,^2\Sigma_u^+$ state.
[b]With potential curve crossing.
[c]Without potential curve crossing.

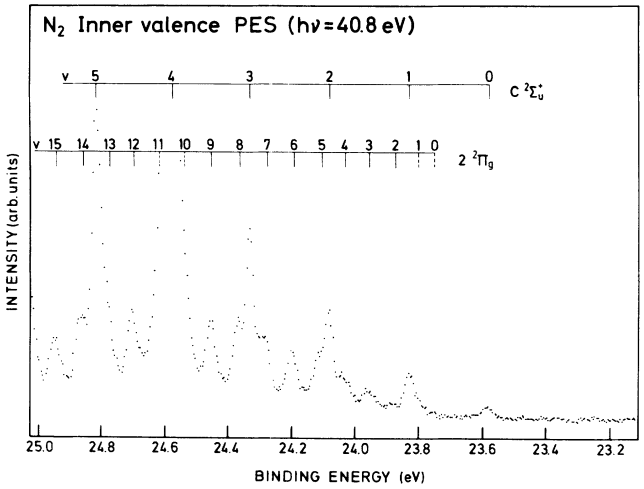


FIG. 3. A recording of the low-energy part of the spectrum in Fig. 2. The vibrational assignment of the low-energy progression has been made by comparison to the vibrational spacings obtained in the calculations. The $v=0$ and 1 components of the $2\,^2\Pi_g$ state are not clearly seen and are therefore indicated by dotted lines.

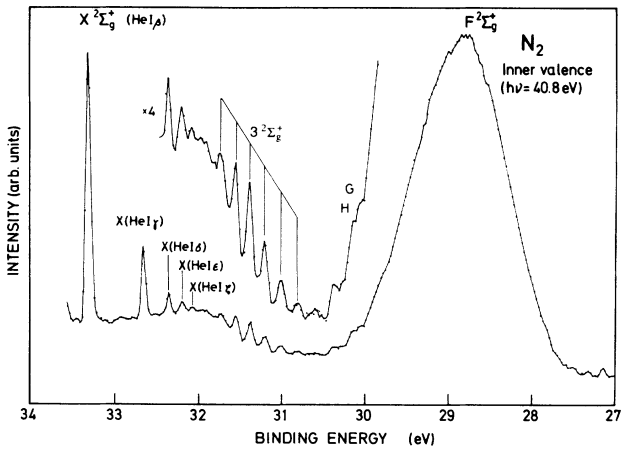


FIG. 5. The inner-valence photoelectron spectrum of $N_2$ between 27 and 33.5 eV excited by monochromatic He II $\alpha$ radiation. A vibrational progression can be discerned in the photoelectron band associated with transitions to the $3\,^2\Sigma_g^+$ cationic state. Due to scattered radiation, the remaining He I radiation gives rise to observable transitions to the $X$ state.

components are clearly discernible. The intensity in the beginning of the band is very low, which makes an identification of the adiabatic transition difficult. However, by comparison with the theoretical results, it seems that the weak feature observed at 23.755 eV can be assigned to this transition. This will be further discussed in the next section.

In Fig. 5 we show a detail of the spectrum in Fig. 1 ranging from 27 to 33.5 eV. The spectrum is dominated by a strong, essentially structureless peak centered around 28.8 eV. In Ref. [4] this structure was ascribed mainly to transitions to the $F\,^2\Sigma_g^+$ state. Since no clear vibrational structure can be observed, the state must have a repulsive potential curve in the Franck-Condon region. This is confirmed by the *ab initio* calculations, as will be discussed below. On the high-binding-energy side of the XPS line another weak feature was observed, which, by comparison to the DES spectrum, was assigned to the $G\,^2\Pi_u$ state. In the present spectrum weak structures can be inferred around 30 eV in Fig. 5, and may correspond to the $G$ and also the $H$ states, which are both expected to appear in this energy region [4].

The band observed in the (31–32)-eV range exhibits a clear vibrational progression (cf. Fig. 5) with spacings of about 180 meV, as indicated by the bar diagram. This shows that the state is bound with a force constant similar to that of the $A$ state in the outer valence region. The energies are collected in Table IV. The intensity increases gradually from the beginning of the band, and the first peak that can be unambiguously associated with this state is observed at 30.8 eV. At lower binding energies

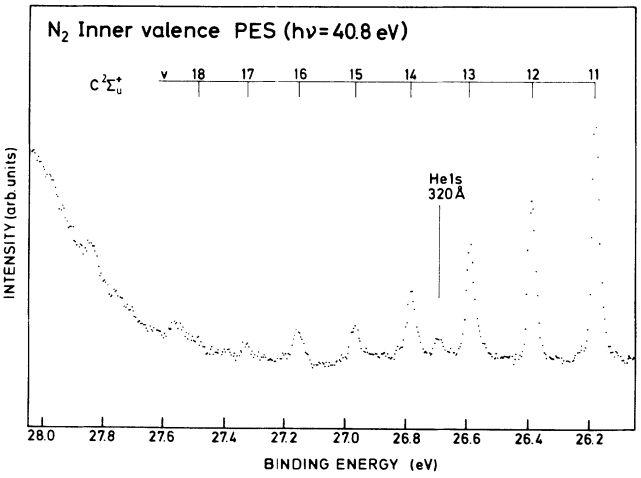


FIG. 4. A recording of the high-energy part of the spectrum in Fig. 2 showing the highest vibrational components associated with transitions to the $C\,^2\Sigma_u^+$ state. The $v=16$ line is broadened compared to the lower lines.

TABLE IV. Vibrational energy levels for the $3\,^2\Sigma_g^+$ state of $N_2^+$ and relative intensities in transitions from the neutral ground state. The vibrational numbers are tentative, since there may be unresolved lines at even lower energies superimposed on the strong band arising from transitions to the $F\,^2\Sigma_g^+$ state.

| Vibrational quantum number $v$ | Binding energy (eV) | Vibrational spacing (meV) | Relative intensity |
|---|---|---|---|
| 0 | 30.815 | | 0.84 |
| 1 | 31.010 | 195 | 1.00 |
| 2 | 31.200 | 190 | 0.70 |
| 3 | 31.375 | 175 | 0.38 |
| 4 | 31.545 | 170 | 0.18 |
| 5 | 31.713 | 168 | 0.079 |

additional features can be observed, but they might rather be related to the complex features seen slightly above 30 eV on the high-energy side of the intense band centered at 28.8 eV. It is therefore not possible to determine the adiabatic ionization energy from the experimental results.

Above 31.9 eV the line structure is diffuse and seems to form a continuous distribution. However, ionization from the $3\sigma_g$ orbital with the He I resonance series starts at about 32 eV, and the presence of these structures makes it difficult to follow the band at higher binding energies.

## V. DISCUSSION

From the experimental information obtained in the present study, it is possible to determine vibrational constants and obtain information on the potential curves in the inner-valence region of $N_2^+$. However, the potential curves are very complex, and we have found that the best representations are provided by the theoretical curves obtained from the MRCI calculations. Figure 6 shows these potential-energy curves obtained in the present study along with the corresponding results of Ref. [13]. The energy values calculated in the present study are collected in Table V.

Most of the inner-valence states in the (20–33)-eV range have deep potential minima located close enough to the Franck-Condon region that vibrational structure should be readily observed in the photoelectron spectrum in direct transitions from the neutral ground state. However, the observed vibrational structure seems to be associated with only a few electronic states, which implies that most states are not appreciably populated in the photoelectron transitions. Since the vibrational structure is well-defined and the calculated vibrational energies are known to be accurate, it is possible to identify these states.

The vibrational constants given for the $C\,^2\Sigma_u^+$ state in Refs. [28, 29] give a good fit only to the observed vibrational energies for quantum numbers $v \leq 10$. The disagreement at higher energies seems to result from the use of a Morse potential curve, which is not capable of describing the observations accurately in the high-energy range.

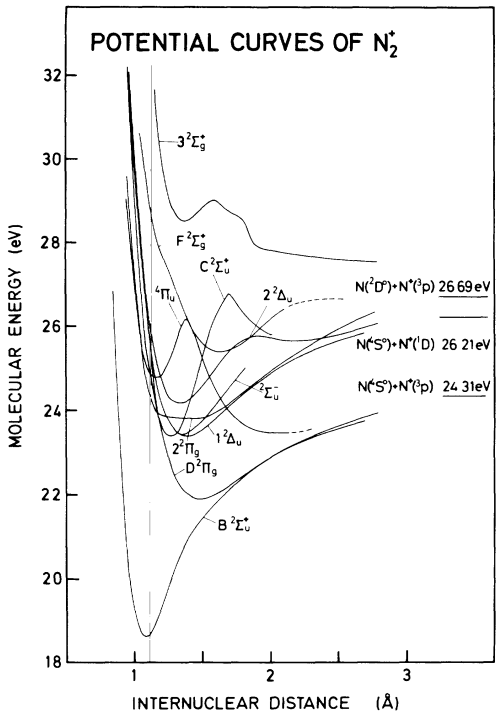


FIG. 6. Theoretical potential curves obtained in the present study and in Ref. [13] in the energy range between 18 and 32 eV. The three lowest dissociation limits are also included. The $B\,^2\Sigma_u^+$, $D\,^2\Pi_g$, and $^4\Pi_u$ states are connected to the lowest limit, whereas all the other curves go to the dissociation limit at 26.69 eV. The energy scale refers to the $v=0$ level of the neutral ground state. The vertical line is drawn at the center of the Franck-Condon region.

TABLE V. Theoretical potential energies (in hartrees) obtained in the present study for the $D\,^2\Pi_g$, $2\,^2\Pi_g$, $F\,^2\Sigma_g^+$, and $3\,^2\Sigma_g^+$ states of $N_2^+$.

| $R$ (a.u.) | $D\,^2\Pi_g$ | $2\,^2\Pi_g$ | $F\,^2\Sigma_g^+$ | $3\,^2\Sigma_g^+$ |
|---|---|---|---|---|
| 1.8 | −108.131 600 | −108.303 122 | −108.115 903 | |
| 2.0 | −108.364 926 | −108.443 764 | −108.278 932 | −108.079 186 |
| 2.2 | −108.484 055 | −108.494 490 | −108.347 426 | −108.233 485 |
| 2.4 | −108.542 206 | −108.498 511 | −108.379 692 | −108.313 737 |
| 2.6 | −108.564 429 | −108.498 524 | −108.412 505 | −108.326 976 |
| 2.8 | −108.569 384 | −108.499 753 | −108.434 781 | −108.316 217 |
| 2.9 | −108.568 318 | −108.498 145 | | |
| 3.0 | −108.565 857 | −108.495 286 | −108.443 443 | −108.307 480 |
| 3.2 | −108.558 544 | −108.486 745 | −108.442 388 | −108.318 307 |
| 3.4 | −108.549 873 | −108.476 594 | −108.435 357 | −108.325 345 |
| 3.6 | −108.541 049 | −108.465 971 | −108.425 600 | −108.348 646 |
| 4.0 | −108.525 004 | −108.446 787 | −108.404 807 | |
| 5.0 | −108.499 342 | −108.412 247 | | −108.360 610 |
| 6.0 | −108.490 647 | −108.398 770 | | |
| 8.0 | −108.487 779 | −108.392 366 | | |
| 10.0 | −108.487 386 | −108.391 738 | | |

The "dissociation limit" that can be obtained for the $C$ state from the vibrational constants lies above 30 eV, and corresponds to a very high vibrational quantum number. However, due to the presence of a perturbing state, the adiabatic potential curve has a barrier maximum at 1.7 Å, another local minimum at about 2.2 Å, and then approaches the dissociation limit 26.69 eV [13], where the molecule is separated into a $N(^2D)+N^+(^3P)$ system (cf. Fig. 6). The barrier maximum is located approximately 3.34 eV above the $v=0$ level, according to the *ab initio* calculations of Ref. [13]. Using the experimental adiabatic binding energy 25.583 eV, the barrier maximum is thus expected to occur at 26.93 eV, which is approximately 0.24 eV above the dissociation limit. This barrier maximum corresponds essentially to the position of the $v=15$ level in the experimental spectrum, while the highest observed vibrational level, $v=18$, appears at a much higher energy, 27.5 eV, which is 0.8 eV above the dissociation limit. However, as mentioned above, the $v=16$ line, which is well resolved and recorded with good statistics, is much broader than the $v=15$ line, suggesting that its lifetime is much reduced, presumably due to dissociation. This may be explained if it is assumed that the $v=16$ level is located at the top of the barrier maximum and that the structures labeled $v=17$ and 18 correspond to resonances located above the barrier.

The second vibrational progression in the (23–27)-eV range has spacings that are somewhat similar to those obtained previously for the $D\,^2\Pi_g$ state [28,29] but differ much from theoretical results for the $^2\Sigma_u^-$ and $1\,^2\Delta_u$ states, which are known to lie in the same energy range [13] (cf. also Fig. 6). Thus, an assignment of this progression in terms of the two latter electronic states can be ruled out. We have previously ascribed this vibrational progression to the $D$ state [4] by a comparison to results from DES and XPS as well as the small vibrational spacings obtained earlier for this state. However, the dissociation limit of the $D$ state occurs at 24.31 eV, where the molecular cation breaks up into a $N(^4S°)+N^+(^3P)$ system, while in the present investigation the vibrational progression can be followed up to above 26 eV. This implies that if the vibrational progression were due to the $D$ state, this state must have a potential barrier of a least 1.7 eV. One reason to carry out the CI calculations of the potential curves and vibrational structure associated with the $D$ state, and also the next state of the same symmetry, $^2\Pi_g$, was to find out whether this could be possible.

The interesting part of Fig. 6 is shown in more detail in Fig. 7. As can be seen, no potential barrier is predicted, and the curve of the $D$ state connects smoothly to the dissociation limit, as indicated also by the curve given in Refs. [13,23]. Thus, it seems impossible to associate the observed vibrational structure with transitions to the $D$ state. On the other hand, the potential curve of the perturbing $2\,^2\Pi_g$ state crosses the Franck-Condon region in the range where the vibrational structures are observed in the spectrum. Furthermore, the vibrational spacings derived for this potential resemble closely the observed spacings, as can be seen in Table III. Two sets of theoretical values are given, corresponding to the results obtained if curve crossing is allowed (diabatic curves) and if

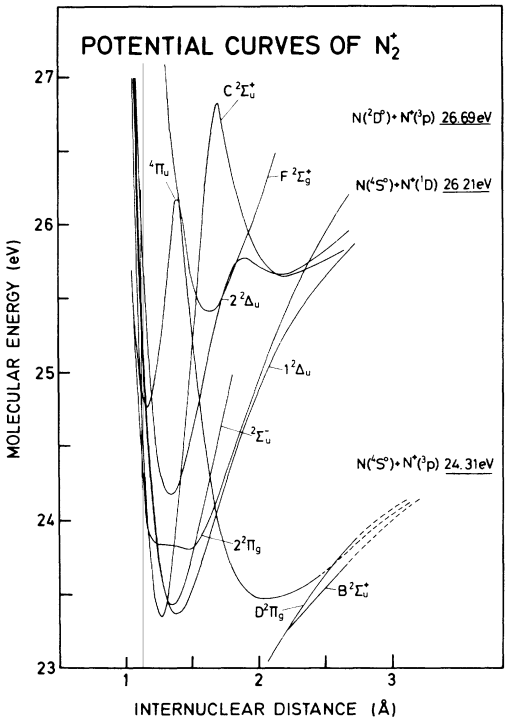


FIG. 7. An enlargement of the potential curves of Fig. 6 in the region between 23 and 27 eV. The vertical line is drawn at the center of the Franck-Condon region.

crossing is not allowed (adiabatic curves). From these observations, and the fact that no other potential curve in this energy range gives rise to such small vibrational spacings, it seems obvious that the observed progression must be associated with transitions to the $2\,^2\Pi_g$ state. It may also be noted that the spacings calculated when allowing a crossing with the $D$ state agree better with the experimental results than those obtained for the adiabatic curve. Thus, it seems that the energy levels are determined primarily by the wide potential curve obtained when curve crossing is accepted. The resulting theoretical potential curves for this situation are shown separately in Fig. 8, along with the theoretical potential curve of the $C\,^2\Sigma_u^+$ state [13]. Curve crossings of this kind have been found also in the case of the inner-valence photoelectron spectrum of $O_2$ [30].

The first few calculated vibrational spacings of this state are very small, and the spacings increase gradually towards a maximum at about $v=8$. As was mentioned above, the experimental spectrum seems to show a similar behavior, exhibiting increase in the vibrational spacings from the beginning of the band. This unusual behavior is explained by the shape of the potential curve, which is almost flat at the bottom (cf. Figs. 7 and 8), as was found also in the calculations of Ref. [10]. From the comparison between the experimental and theoretical vibrational energies, we associate the very weak feature observed at 23.755 eV with the adiabatic transition to the $2\,^2\Pi_g$ state, which gives a 0-1 splitting of 54 meV. However, since the vibrational structure belonging to the

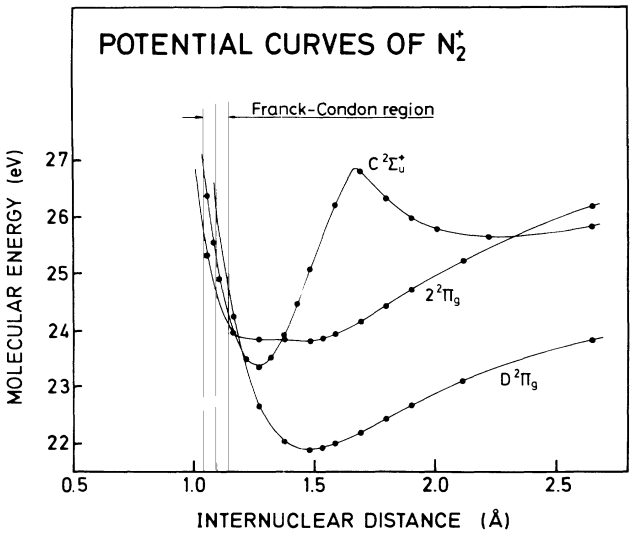


FIG. 8. Theoretical potential curves of the $D\,^2\Pi_g$ and $2\,^2\Pi_g$ states obtained in the present study and of the $C\,^2\Sigma_u^+$ state from Ref. [13]. The dots show the calculated data points. The Franck-Condon region for transitions from the neutral ground state is also shown.

$2\,^2\Pi_g$ state is not very well defined in this part of the spectrum, this assignment is considered tentative.

The energy scales of Figs. 6–8 refer to the $v=0$ level of the neutral ground state. The absolute energies of the potential curves were obtained by adjusting the energy minimum of the $B\,^2\Sigma_g^+$ state given in Ref. [13] to the experimental value 18.601 eV, obtained from Ref. [28] by adding $T_e=3.157$ eV to the adiabatic binding energy 15.580 eV of the $X\,^2\Sigma_g^+$ cationic state, and accounting for the zero-point energy of this state. The energy positions of the potential curves obtained in this manner fit very well with the observed vibrational structure. The deviations are in all cases less than 100 meV.

Figure 8 is useful also for discussing the intensity distributions of the photoelectron bands observed in the region around 25 eV. In particular, the center of the Franck-Condon region should cross the potential curve approximately at the position of the maximum intensity. Thus, if all the three states in figure are considered, it is obvious that the first intensity maximum should be observed for the $2\,^2\Pi_g$ state at about 24.7 eV, the second for the $C\,^2\Sigma_u^+$ state at 25.3 eV, and the third for the $D\,^2\Pi_g$ state at about 26 eV. As can be seen from Tables II and III, the observed intensity maxima of the $2\,^2\Pi_g$ and $C\,^2\Sigma_u^+$ states occur at about 24.8 and 25.5 eV, respectively, so the agreement between experiment and theory is almost perfect. Concerning the $D$ state, the center of the Franck-Condon region crosses the potential curve far above the dissociation limit. Photoelectron transitions to this state would therefore be expected to give rise to a structureless band in the range around 26 eV. Thus, what appears to be an enhancement of the background in this energy range of the spectrum probably reflects transitions to the $D\,^2\Pi_g$ state. Similarly, one would expect to observe a continuous intensity distribution of $N^+$ in the photoion spectrum, with maximum intensity about 26 eV. In fact, it seems that the line structure of this spectrum, associated with predissociation from the vibrational levels of the $C\,^2\Sigma_u^+$ state and from preceding Rydberg states [27], is indeed superimposed on such an intensity distribution. It may be noticed from Figs. 6 and 7 and the potential curves presented in Refs. [10], [11], and [13] that the $D$ state is the only state that is dissociative in this energy range, which excludes other assignments.

Although the vibrational structure favors a description in terms of crossed potential curves between the $D\,^2\Pi_g$ and $2\,^2\Pi_g$ states, as shown in Fig. 7, it is clear that there is some interaction between the states. This implies that the $2\,^2\Pi_g$ state interacts with the dissociation continuum of the $D\,^2\Pi_g$ state, which could thus led to enhanced production of $N^+$ ions at the positions of the vibrational levels. An interaction of this kind was previously proposed to be responsible for predissociation of the $C\,^2\Sigma_u^+$ state, which is coupled to the dissociation continuum via interaction with the $B\,^2\Sigma_u^+$ state in the repulsive part of its potential curve [11]. A comparison with the photoion spectrum [27] seems to reveal some very weak features at the expected energies of the $2\,^2\Pi_g$ state. Possibly, the enhanced width of the photoelectron lines associated with this state may suggest that the lifetime towards dissociation is short.

The structures in the spectrum associated with the $D\,^2\Pi_g$ and $2\,^2\Pi_g$ final states can most probably be characterized as initial-state electron correlation satellites. According to calculations [6], monopole shakeup transitions cannot be observed in the present energy range, and since there is no single hole state of $^2\Pi_g$ symmetry, it is difficult to envision a final-state electron correlation effect. Inclusion of electron correlation in the initial state, on the other hand, mixes in some $1\pi_g^2$ character in the wave function, and under such circumstances states of $^2\Pi_g$ symmetry can be reached in photoelectron transitions. This was discussed in Refs. [25], [26], and [31], where intensity coefficients of less than 0.01 (but not zero) were obtained for both states of $^2\Pi_g$ symmetry in this energy range, in qualitative agreement with the present results. Another effect that could be responsible for some intensity in the spectrum is spin-orbit interactions. However, since this effect is small in the present energy range [32], this is not an obvious mechanism for intensity borrowing. An additional source of intensity could be a weak population of autoionizing states in the 40.8-eV region. Since the presence of such states cannot be excluded at present, this implies that the relative intensity observed in the spectrum gives an upper limit of the intensity generated by the initial-state correlation effect.

As mentioned above, the band associated with the $F\,^2\Sigma_g^+$ state does not show much structure, which suggests that this state has a potential curve that is dissociative in the Franck-Condon region between 28 and 30 eV. This is confirmed by the present calculations, as can be seen from Figs. 6 and 7. The crossing between the potential curve and the center of the Franck-Condon region occurs at 28.8 eV, which agrees closely with the intensity

maximum of the photoelectron band, as expected. The potential curve is not repulsive, however, but shows a minimum at an internuclear distance of about 1.6 Å. Since the dissociation limit is 26.7 eV, it seems unlikely that the observed weal features in the beginning and at the end of the photoelectron band reflect vibrational levels of this state. The weak features observed around 30 eV might therefore be associated with the *G* and *H* states, which are expected to appear in this region [4].

In the former study [4], the photoelectron band observed in the (31–32)-eV energy range, which exhibits a vibrational progression, was referred to as the $I\,^2\Sigma_u^+$ state. However, in the present calculations, carried out on electronic states in this energy region, we have not been able to find a bound state with this symmetry. The only state that has been found to have a minimum in the potential is the $3\,^2\Sigma_g^+$ state, and we therefore tentatively assign the structure to this state. The agreement with the experiment is not as good as for the other states in this study.


[1] L. Åsbrink and C. Fridh, Phys. Scr. **9**, 338 (1974).
[2] A. W. Potts and T. A. Williams, J. Electron Spectrosc. **3**, 3 (1974).
[3] S. Krummacher, V. Schmidt, and F. Wuilleumier, J. Phys. B **13**, 3993 (1980).
[4] S. Svensson, M. Carlsson Göthe, A. Nilsson, L. Karlsson, N. Mårtensson, and U. Gelius, Phys. Scr. **44**, 184 (1991).
[5] W. Eberhardt, E. W. Plummer, I.-W. Lyo, R. Murphy, R. Carr, and W. K. Ford, J. Phys. (Paris) Colloq. **48**, Suppl. 12, C9-697 (1987).
[6] H. Ågren, R. Arneberg, J. Müller, and R. Manne, Chem. Phys. **83**, 53 (1984).
[7] J. A. R. Samson, G. N. Haddad, and J. L. Gardner, J. Phys. B **10**, 1749 (1977).
[8] P. Baltzer, M. Carlsson-Göthe, B. Wannberg, and L. Karlsson, Rev. Sci. Instrum. **62**, 630 (1990).
[9] A. Andersen and E. W. Thulstrup, J. Phys. B **6**, L211 (1973).
[10] E. W. Thulstrup and A. Andersen, J. Phys. B **8**, 965 (1975).
[11] A. L. Roche and H. Lefebvre-Brion, Chem. Phys. Lett. **32**, 155 (1975).
[12] S. R. Langhoff, C. W. Bauschlicher, Jr., and H. Partridge, J. Chem. Phys. **87**, 4716 (1987).
[13] S. R. Langhoff and C. W. Bauschlicher, Jr., J. Chem. Phys. **88**, 329 (1988).
[14] P. Baltzer, B. Wannberg, and M. Carlsson Göthe, Rev. Sci. Instrum. **62**, 643 (1990).
[15] P. Baltzer, L. Karlsson, and B. Wannberg (unpublished).
[16] P. Baltzer and L. Karlsson, Uppsala University Institute of Physics Report No. UUIP-1211, 1989 (unpublished).
[17] P. E. M. Siegbahn, J. Almlöf, A. Heiberg, and B. O. Roos, J. Chem. Phys. **74**, 2384 (1981).
[18] P. E. M. Siegbahn, Int. J. Quantum Chem. **23**, 1869 (1983).
[19] S. Huzinaga, J. Chem. Phys. **42**, 1293 (1965).
[20] T. H. Dunning, J. Chem. Phys. **55**, 716 (1971).
[21] B. Wannberg, D. Nordfors, K. L. Tan, L. Karlsson, and L. Mattsson, J. Electron Spectrosc. **47**, 147 (1988).
[22] L. Karlsson, S. Svensson, and A. Svensson, J. Phys. B. **22**, 3423 (1989).
[23] F. R. Gilmore, The Rand Corp., Mem. No. RM-4034-PR, 1964 (unpublished).
[24] M. Okuda and N. Jonathan, J. Electron Spectrosc. **3**, 19 (1974).
[25] L. S. Cederbaum and W. Domcke, Adv. Chem. Phys. **36**, 205 (1977).
[26] J. Schirmer and O. Walter, Chem. Phys. **78**, 201 (1983).
[27] L. E. Berg, P. Erman, E. Källne, S. Sorensen, and G. Sundström, Phys. Scr. **44**, 131 (1991).
[28] K. P. Huber and G. Herzberg, *Molecular Spectra and Molecular Structure IV. Constants of Diatomic Molecules* (Van Nostrand Reinhold, New York, 1979).
[29] A. Lofthus and P. H. Krupenie, J. Phys. Chem. Ref. Data **6**, 113 (1977).
[30] P. Baltzer, B. Wannberg, L. Karlsson, and M. Carlsson Göthe, Phys. Rev. A **45**, 4374 (1992).
[31] L. S. Cederbaum, W. Domcke, J. Schirmer, and W. von Niessen, Adv. Chem. Phys. **65**, 115 (1986).
[32] A. J. Lorquet and J. C. Lorquet, Chem. Phys. Lett. **26**, 138 (1974).